# EFFECT OF ANNEALING TEMPERATURE ON TEXTURE OF COLD-ROLLED $Ni_{47}Ti_{44}Nb_9$ SHEET[1]

Yang, Guanjun*† Xie, Liying* Hu, Wenying*
Deng, Ju* Hao, Shiming†
* *Northwest Institute for Nonferrous Metal Research, Baoji 721014*
† *Northeastern University, Shenyang 110006*

**ABSTRACT** The textures of the cold-rolled and annealed $Ni_{47}Ti_{44}Nb_9$ sheets have been studied using the orientation distribution function (ODF) method. The results indicated that the cold-rolled sheet showed a dominant $\{100\}_p$ face texture, and its recrystallization textures could be described with $\{001\}\langle 100\rangle_p$. Moreover, when the cold-rolled sheet was annealed at 700 or 850 C, there occurred abnormal coarsening, thus forming a new kind of annealing texture $\{001\}\langle 1\bar{1}0\rangle_p$.

**key words**: annealing temperature $Ni_{47}Ti_{44}Nb_9$ texture ODF

## 1 INTRODUCTION

It is well known that some of the properties of a polycrystalline material depend on the texture. Especially for shape memory alloys (SMAs), because there exists definite orientation relationship between the lattices of the austenite ($P$) and the martensite ($M$), the shape memory effect (SME) of polycrystalline materials is closely related with the texture. Although people have tried to improve the SME and superelasticity of the TiNi SMAs through controlling the texture types, a great quantity of works need to be done further. Nowadays, only a few papers have been reported on the textures of the SMAs, and the pole figure method is the predominant means used for texture analysis[1-4]. The orientation distribution function (ODF) method is the most effective modern method for texture analysis[5]. So far, few people have used the ODF technique to analyse the textures in the TiNi SMA sheets. The $Ni_{47}Ti_{44}Nb_9$ alloy with good prospects is a SMA of wide hysteresis effect, developed by Raychem Company of America in 1986[6]. The purposes of this paper are to study the textures of the alloy sheet by means of ODF, and to discuss the effect of annealing temperature on the textures.

## 2 EXPERIMENTAL

The test alloy with the nominal composition (at.-%) 47Ni44Ti9Nb was melted by a vacuum induction furnace. After having been homogenized at 850 C for 2 h, the alloy ingots were made into sheets of 1.5 mm thickness through hot forging and cross hot rolling, next annealed at 850 C for 0.5 h, then cold rolled into sheets of 1.0 mm thickness. Six kinds of samples at different conditions were prepared for texture measurements (Table 1).

**Table 1 Samples at different conditions for texture measurement**

| No. | condition |
|---|---|
| R | as cold-rolled |
| A1 | cold rolled+300 C, 30 min+FC* |
| A2 | cold rolled+400 C, 30 min+FC* |
| A3 | cold rolled+550 C, 30 min+FC* |
| A4 | cold rolled+700 C, 30 min+FC* |
| A5 | cold rolled+850 C, 30 min+FC* |

* : FC—furnace cooling.

[1] Received Jun. 20, 1994; accepted in revised form Aug. 8, 1994

The pole figure data were collected on a Philip PW 1700 X-ray diffractometer using $CuK_\alpha$ radiation. The incomplete pole figures in the range $\alpha \leqslant 75°$ were measured using the step scanning method.

From ref. [7], it is known that the $M_s$ temperature of $Ni_{47}Ti_{44}Nb_9$ alloy is $-90$ ℃, and its main constitutional phase is the TiNi phase with $B2$ structure. Therefore, for the six kinds of samples shown in Table 1, the reflection method was used to determine the {002}, {110} and {112} incomplete pole fingures of the $B2$ phase, then Roe method was used to calculate the ODFs[5].

## 3 RESULTS AND DISCUSSION

For *bcc* phases, the orientation characteristics of their dominant textures are mainly reflected on the ODF cross-section patterns with Euler angles $\varphi = 0$ and $\varphi = 45°$. Therefore, only these ODF cross-section patterns were given in this paper.

Fig. 1 shows the constant $\varphi$ cross-section patterns of the grain orientation distribution of the $B2$ phase in the cold-rolled sample. It can be seen that although the one-way cold-rolling was adopted for the alloy sheets, the textures of the cold-rolled sheets retained the characterstics of those of the cross hot-rolled sheets due to the fact that the reduction of the cold-rolling is much smaller than that of the cross hot-rolling and the dominant texture is $\{001\}_p$ face texture. In addition, there also exists $(\bar{1}10)_p$ face texture with small polar density.

Figs. 2～6 show the constant $\varphi$ cross-section patterns of the cold-rolled samples after annealing at 300, 400, 550, 700 and 850 ℃, respectively. It can be seen that annealing changes the texture type of the alloy sheets, and with the changing annealing temperature, the texture type changes correspondingly.

From Fig. 2, it can be seen that after annealing at 300 ℃, the $\{001\}_p$ face texture vanishes, the polar density of the $(\bar{1}10)_p$ face texture decreases, and plate texture forms with $(\bar{1}01)[0\bar{1}0]_p$ and $(\bar{5}53)[\bar{1}\bar{1}0]_p$ as predominant orientations. Moreover, from the $\varphi = 0$ cross-section pattern, it is clear a cubic texture $\{001\}\langle 100\rangle_p$ tends to form after annealing at 300 ℃. When the annealing temperature reaches 400 ℃ (Fig. 3), the regions with maximum polar density correspond to $(\bar{1}05)[0\bar{1}0]_p$ and $(\bar{5}01)[0\bar{1}0]_p$ textures. It is obvious that these textures are unstable, and they will be transformed into cubic textures with increasing temperature. From Fig. 4, it can be seen that when the annealing temperature is raised up to 550 ℃, there occurs substantive change in the texture type. Fig. 4(a) indicates that

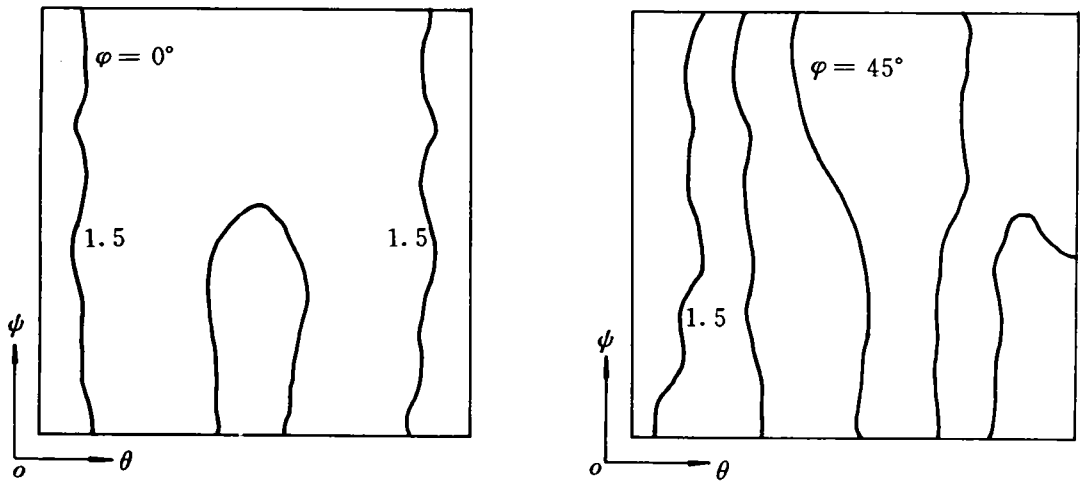


**Fig. 1 Constant $\varphi$ cross-section patterns of $B2$ phase grain orientation distribution in Sample R**

that this sample is typical of the cubic texture $\{001\}\langle 100\rangle_p$, while Fig. 4(b) indicates that the two regions with maximum polar density correspond to $(001)[1\bar{5}0]_p$ and $(001)[\bar{1}\bar{5}0]_p$ textures. If using low indices to express high indices roughly, they can all be expressed with $\{001\}\langle 100\rangle_p$. This means that the texture of Sample A3 is typical of the cubic texture.

Fig. 5 shows the constant $\varphi$ cross-section patterns, of Sample A4. It is clear that when annealed at 700 ℃, there occur drastic changes in the main constituents of the textures. The cubic texture $\{001\}\langle 100\rangle_p$ was damaged and the regions with the maximum polar density corresponding to $\{001\}\langle 100\rangle_p$ transforms to $(\bar{1}15)[5\bar{5}2]_p$ and $(\bar{1}05)[5\bar{4}1]_p$ plate textures. As compared with Sample A4, there occur no big changes in the main component of Sample A5 annealed at 850 ℃ (Fig. 6)

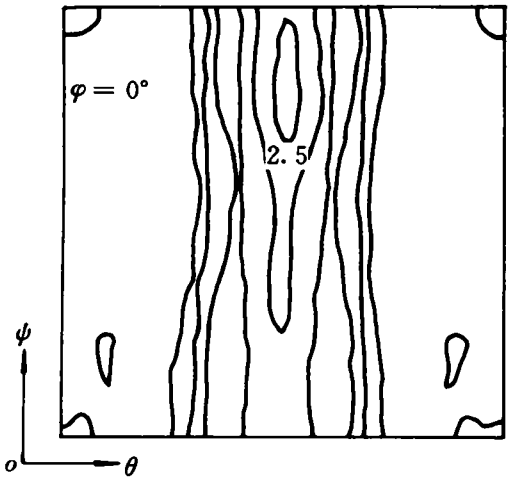


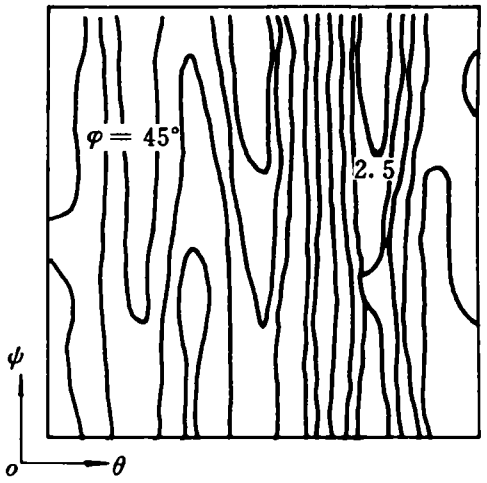


**Fig. 2 Constant $\varphi$ cross-section patterns of $B2$ phase grain orientation distribution in Sample A1(300 ℃, 30 min)**

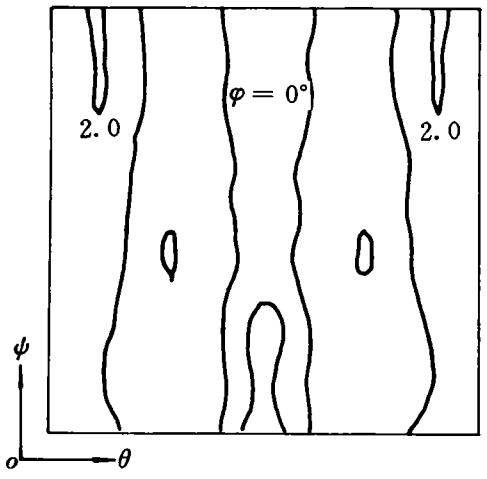


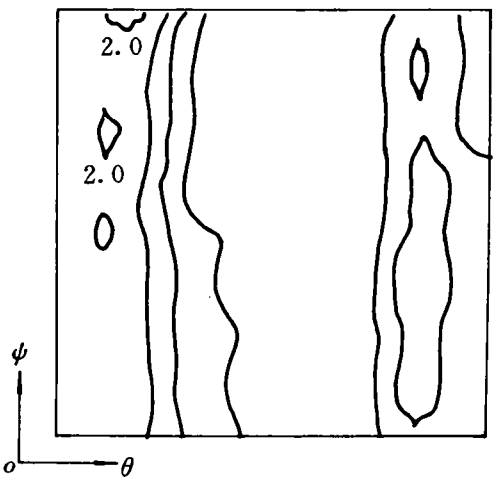


**Fig. 3 Constant $\varphi$ cross-section patterns of $B2$ phase grain orientation distribution in Sample A2(400 ℃, 30 min)**

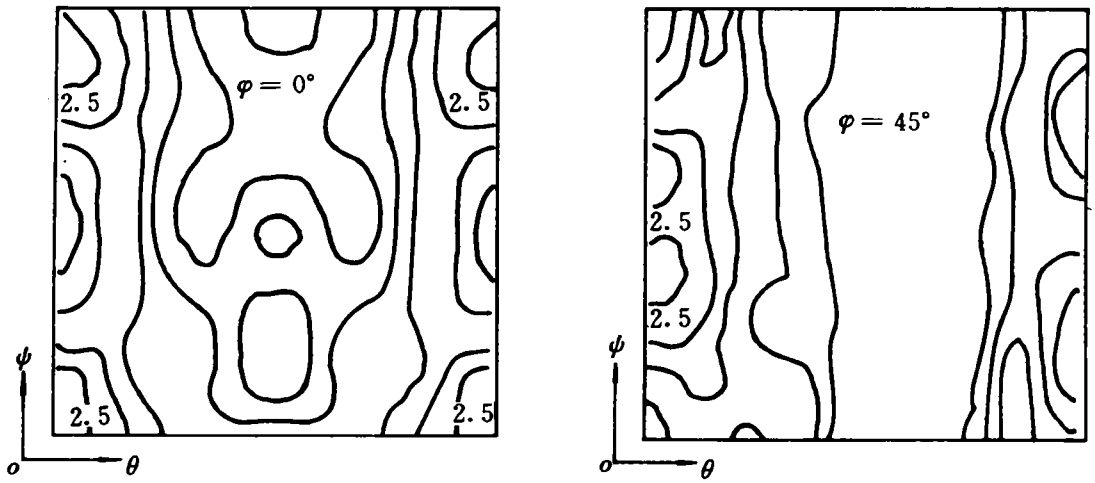


**Fig. 4 Constant φ cross-section patterns of *B2* phase grain orientation distribution in Sample A3(550 ℃, 30 min)**

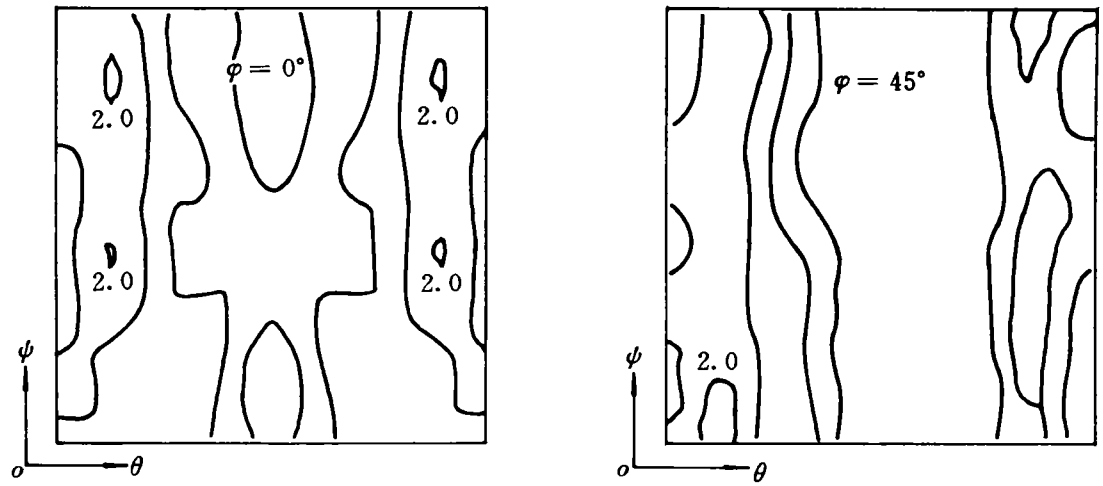


**Fig. 5 Constant φ cross-section patterns of *B2* phase grain orientation distribution in Sample A4(700 ℃, 30 min)**

6), only the four corresponding regions with maximum polar densities in the $\varphi = 0°$ cross-section pattern of Sample A4 converge into two regions along $\psi$ angles and there forms the predominant $\{10\bar{5}\}\langle 5\bar{5}1\rangle_p$ texture. Furthermore, the intensity of the $(\bar{1}15)[5\bar{5}2]_p$ texture decreases slightly. If using low indices to express the textures roughly, the $\{10\bar{5}\}\langle 5\bar{5}1\rangle_p$ and $(\bar{1}15)[5\bar{5}2]_p$ textures can all be expressed by $\{001\}\langle 1\bar{1}0\rangle_p$. Thus, it can be considered that the texture of Sample A5 is $\{001\}\langle 1\bar{1}0\rangle_p$.

In addition, it should be noted that by comparing the constant φ cross-section patterns of Sample A4 with that of Sample A5, it can be seen that the orientation distribution patterns are very similar, which indicates that the dominant texture components of the two samples are of no essential distinction, namely the same.

Gorelik[8] indicated that the complex deformation in rolling can be expressed conditionally by the tension along the rolling direc-

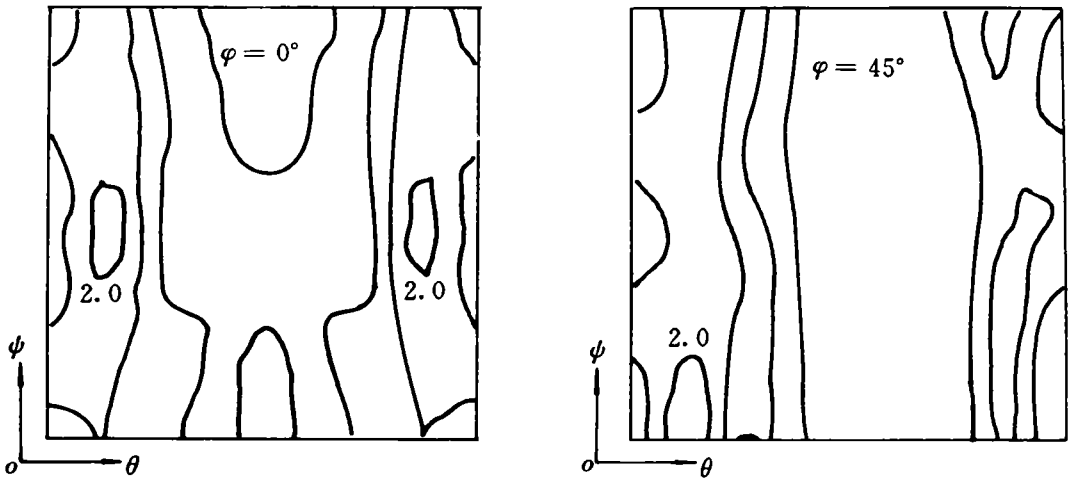


**Fig. 6 Constant φ cross-section patterns of *B*2 phase grain orientation distribution in Sample A5(850 C, 30 min)**

tion and the compression perpendicular to the rolling plane. When a *bcc* metal is under tension, its〈110〉direction is parallel to the tensile axis, namely the rolling direction. This means that when the metal is rolled the compression direction is perpendicular to a plane containing 〈110〉directions. Because of symmetry of lattices of *bcc* metals a couple of equivalent planes of the 〈110〉group perpendicular to each other participate the slip at the same time. The {110}〈111〉system is the primary slip system of *bcc* metals, slip firstly takes place on the {110}planes in the 〈111〉directions, finally in the 〈100〉directions. For the other pair of {110}planes, the slip also takes place in the 〈001〉directions perpendicular to former directions. This implies that the slip should take place on the planes containing two 〈001〉directions and a 〈110〉direction. The {001}planes can satisfy this condition, thus the planes must be perpendicular to the compression axis, namely parallel to the rolling plane. This is the origin of the stable {001}〈110〉texture found in *bcc* metals. However, when the *bcc* metals are deformed lots of slip systems are set in motion, thus there exist several types of textures. The test alloy is mainly composed of the ordered *B*2 phase, whose deformation was completed using the cross hot rolling and one-way cold rolling. Because the reduction of hot rolling is larger than that of cold rolling, there occur no preferred orientations on the rolling plane. Therefore, the $\{001\}_p$ planes of most *B*2 phase in the test alloy parallel to the rolling plane, the $(\bar{1}10)_p$ planes of a few grains also parallel to the rolling plane.

After annealing, the materials with deformation textures usually exhibit preferred orientations, namely there form the so-called recrystallization textures or annealing textures. There are two kinds of theories[9] on the formation of the recrystallization textures: One is the directional nucleation theory which believes that in recrystallization only those sub-grains with most favourable orientations can grow and act as recrystallization nuclei, finally become recrystallized grains basically of the same orientation. The main shortcoming of this theory is that it cannot explain the texture development in recrystallization frequently met in practice. Therefore, it is not of universal significance. The other is the directional growth theory which believes that subgrains with any orientations all can form crystals, but only those with the most favourable orientations have highest growth rates and the grains with other orientations were eliminated

in growth competition because of small grain boundary migration rates. Therefore, the recrystallization textures are determined by the orientation along which the grains grow fastest.

If the materials with deformation textures are annealed, developments of texture are likely to be as follows: (1) The deformation texture retains after annealing. (2) The deformation texture will completely or partially be replaced by annealing textures composed of one or several different components. In many cases, the textures forming in the early stage of the recrystallization are replaced by other textures which appear at the late stage of the recrystallization. (3) The deformation textures will be replaced completely or partially by new grains of arbitrary orientations. This case is not as general as the former two. By summing up the above-mentioned experimental results, it can be found that the directional growth theory plays an important role in the development of textures.

When annealed at 300 or 400 C, the main components of the textures are at the unstable stage in the development of textures. Because the annealing temperatures were low, there merely occurred polymerization and sub-grain merging. In spite of this, there still occur large changes in the textures. When annealed at 550 C, there occured complete recrystallization, and the grains with $\{001\}\langle 100\rangle$ orientation had highest interface transfer rates and formed a typical recrystallization texture, e. g. cubic $\{001\}\langle 100\rangle_p$ texture. This also shows that the recrystallization temperature of the $Ni_{47}Ti_{44}Nb_9$ alloy is in the range of 400～550 C, which is consistent with the guess proposed by Piao *et al* [10].

When the annealing temperature is raised up to 700 C or 850 C, because these temperatures are much higher than the recrystallization temperature of the alloy, besides recrystallization, a few grains abnormally grow in the process of annealing. This kind of grain growth is a process that the large grains with small curvatures swallow up the small ones with large curvatures. At this time, the grains with $\{001\}\langle 1\bar{1}0\rangle$ orientation appears speed-up growth, thus forming a new kind of annealing texture—secondary recrystallization texture $\{001\}\langle 1\bar{1}0\rangle_p$.

## 4 SUMMARY

The main texture component of the cold-rolled $Ni_{47}Ti_{44}Nb_9$ sheet is $\{001\}_p$ face texture. Annealed at 300 or 400 C, the recovery process led to the texture change. Annealed at 550 C, recrystallization occurred in the cold-rolled sheet, and formed a typical recrystallization texture $\{001\}\langle 100\rangle_p$. When the annealing temperature was raised up to 700 or 850 C, besides recrystallization, a few grains abnormally grow, thus forming secondary recrystallization texture $\{001\}\langle 1\bar{1}0\rangle_p$.

## REFFRENCES

1 De Lange, R G; Zijderveld, J A. Appl Phys, 1986, 39: 2195.
2 Eucken, S; Hirsch, J. Mater Sci Forum, 1990, 56—58: 487.
3 Li, D Y; Wu, X F; Ko T. Acta Metall Mater, 1990, 38:19.
4 Mulder J H; Thoma, P E; Beyer J. Z Metallkd, 1993, 84:501.
5 Liang, Zhide; Xu, Jiazhen; Wang, Fu. Three-Dimensional Orientation Analysis Technique of Texture Materials. Shenyang: Northeastern University Press, 1986. 36.
6 Melton, K N; Simpson, J; Duerig, T W. In: Proc Int Conf on Martensitic Transformation ICOMAT—86. Nara: Japan Institute of Metals, 1986. 1053.
7 Zhang, C S *et al*. Materials Chemistry and Physics, 1991, 28:43.
8 Gorelik, S S; Tong, Jianmin (trans). Recrystallization in Metals and Alloys. Beijing: Machinery Industry Press, 1985. 52.
9 Deng, Zhiqian; Zhou, Shanchu. Metallic Materials and Heat-treatment. Changsha: Central South University of Technology Press, 1989. 12.
10 Piao, M; Miyaziki, S; Otsuka, K. Mater Trans, JIM, 1992, 33:346.